Tectonophysics xxx (2009) xxx–xxx

Contents lists available at ScienceDirect

Tectonophysics

journal homepage: www.elsevier.com/locate/tecto

Balance of seismic moment in the Songpan-Ganze region, eastern Tibet: Implications for the 2008 Great Wenchuan earthquake

Hui Wang [a,b,*], Mian Liu [b], Xuhui Shen [a], Jie Liu [c]

[a] Institute of Earthquake Science, China Earthquake Administration, Beijing 100036, China
[b] Department of Geological Sciences, University of Missouri, Columbia, MO 65211, USA
[c] China Earthquake Network Center, China Earthquake Administration, Beijing 100045, China

ARTICLE INFO

Article history:
Received 17 February 2009
Received in revised form 15 September 2009
Accepted 25 September 2009
Available online xxxx

Keywords:
Songpan-Ganze region
Great Wenchuan earthquake
Slip rate
Seismic moment
Seismic hazard

ABSTRACT

The 12 May 2008 Wenchuan earthquake (Ms 8.0) occurred on the Longmen Shan fault zone, where slip rates are low and earthquakes are infrequent in comparison with other major fault zones in the Songpan-Ganze region, eastern Tibet. We have investigated the evolution of strain energy along major faults in this region by comparing the accumulation and release of seismic moment. First, we calculated the slip rates on the Longmen Shan and other major faults in the region using a three-dimensional regional-scale block model, constrained by the latest GPS data. On the Longmen Shan fault, the predicted right-lateral and dip-slip rates are respectively 1.7 ± 0.8 mm/year and 1.2 ± 1.0 mm/year along the southwestern segments, and 1.4 ± 1.1 mm/year and 3.3 ± 1.3 mm/year on the northeastern segments. These slip rates are one order of magnitude lower than those on the Xianshuihe fault and other faults in the region. Second, using the earthquake catalog, we estimated the scalar moment released on major faults in the Songpan-Ganze region between 1879 and 2007. The released seismic moment was ~63% of the regional scalar moment accumulated during this period. The moment deficits were found mainly on the western Xianshuihe and eastern Kunlun faults. The eastern Xianshuihe fault has been a focus of studies because of the high slip rates and frequent earthquakes, but a sequence of major quakes there since 1893 has reduced the moment deficit to 3.68×10^{19} N m, barely enough for a Mw 7.0 event. It takes the Longmen Shan fault more than 1000 years to accumulate the seismic moment (1.15×10^{21} N m) released during the 2008 Great Wenchuan earthquake, hence we conclude that a repeat of great earthquakes on the ruptured segment of the Longmen Shan fault is unlikely in the next few hundred years, but the unruptured southwestern segment of the Longmen Shan fault is capable of producing a Mw 7.7 earthquake in the next 50 years.

1. Introduction

The 12 May 2008 Wenchuan earthquake (Ms 8.0) killed more than 70,000 people and injured hundreds of thousands. The earthquake ruptured more than 250 km along the Longmen Shan fault zone (Zhang et al., 2008) (Fig. 1). The maximum coseismic slip was more than 9.0 m (Ji, 2008).

The Great Wenchuan earthquake occurred in the Songpan-Ganze region of eastern Tibetan Plateau. The Songpan-Ganze region is bounded by the eastern Kunlun fault, the Xianshuihe fault, and the Longmen Shan-Min Shan fault (Fig. 1). The eastward extrusion of the Tibetan crust is accommodated here by the left-lateral Kunlun and Xianshuihe faults, and resisted by the rigid Sichuan block (Allen et al., 1991; Molnar and Tapponnier, 1977; Replumaz and Tapponnier, 2003; Royden et al., 2008; Tapponnier et al., 2001; Wang et al., 2008a). The Longmen Shan fault zone is the boundary between the Tibetan Plateau and the Sichuan block; over this fault zone crustal shortening is absorbed. Both geological and geodetic data show slip rates on the Longmen Shan fault to be a few mm per year, about one order of magnitude lower than those on the Kunlun and Xianshuihe faults (Burchfiel et al., 1995; Burchfiel et al., 2008; Densmore et al., 2007; Wallis et al., 2003; Zhou et al., 2007).

Hence the 2008 Great Wenchuan earthquake was somewhat surprising, although large earthquakes are frequent in the Songpan-Ganze region, where more than 50 M≥6.0 events are documented "(Division of Earthquake Monitoring and Prediction, S.S.B, 1995; Division of Earthquake Monitoring and Prediction, C.S.B, 1999). Most of these quakes occurred on the Kunlun fault and the Xianshuihe fault. The Longmen Shan fault zone has been seismically quiescent before the Great Wenchuan earthquake in 2008.

Seismic activity is a process of energy accumulation and release. To understand the occurrence of the Great Wenchuan earthquake and its impact on regional earthquake hazards, we have compared seismic moments released by earthquakes on the Longmen Shan and other faults with the predicted moment accumulation on these faults. First, we calculated the accumulation of scalar moments based on fault slip

* Corresponding author. Institute of Earthquake Science, China Earthquake Administration, Beijing 100036, China. Tel.: +86 10 88015551.
E-mail address: wanghui500@gmail.com (H. Wang).

0040-1951/$ – see front matter © 2009 Elsevier B.V. All rights reserved.
doi:10.1016/j.tecto.2009.09.022

Please cite this article as: Wang, H., et al., Balance of seismic moment in the Songpan-Ganze region, eastern Tibet: Implications for the 2008 Great Wenchuan earthquake, Tectonophysics (2009), doi:10.1016/j.tecto.2009.09.022

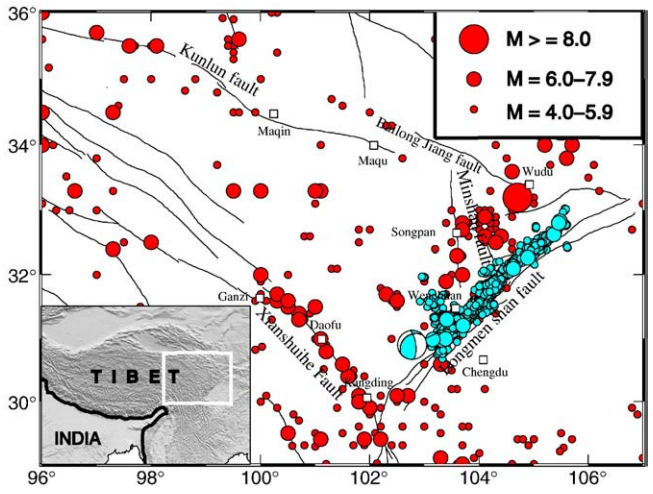

Fig. 1. Major faults and seismicity of the Songpan-Ganze region, eastern Tibetan Plateau; location is shown in the inset. Red circles are historical earthquakes. Blue circle are the main shock of the 2008 Great Wenchuan earthquake and the aftershocks during 5/12–11/20, 2008. (For interpretation of the references to color in this figure legend, the reader is referred to the web version of this article.)

rates, which are calculated from a regional-scale elastic block model constrained by the latest GPS data. Second, we estimated the release of seismic moment based on historical and instrumental earthquake catalogs. Finally, we determined the moment deficit and its distribution, and discussed the implications for the occurrence of the Great Wenchuan earthquake and its impact on the regional earthquake hazards.

2. Fault slip rates and moment accumulation in the Tibetan Plateau

Slip rates are the basis for assessing seismic potential on host faults, and can be determined from active tectonic studies and geodetic measurements. Slip rates derived from active tectonic or neotectonic studies provide long-term average values; many of such studies have been taken in eastern Tibet (Allen et al., 1991; Burchfiel et al., 1995; Deng et al., 2002; Densmore et al., 2007; Van der Woerd et al., 2000). The errors associated with the exposure age of samples may partly explain the large discrepancies among different studies (He et al., 2003; Liu et al., 2000). Furthermore, geological slip rates are available only for a small number of faults and fault sites, inadequate for constraining a regional-scale model. For this reason, we use the Global Positioning System (GPS) data as our primary constraints.

2.1. GPS velocity field in the Tibetan Plateau

The earliest GPS survey in the Tibetan Plateau may date back to 1991, with 12 GPS sites in the southeastern borderland of the Tibetan Plateau. Survey results indicated slow deformation (<3 mm/year) in the Longmen Shan-Min Shan region (Chen et al., 2000; King et al., 1997). Shen et al. (2000) used 84 GPS site velocities, mainly located in North China, to study the contemporary crustal deformation in east Asia. Wang et al. (2001) later collected 354 site velocities in the Chinese mainland. They showed that the deformation of the Tibetan Plateau and its vicinity accommodates most of India's penetration into Eurasia. Zhang et al. (2004) synthesized 553 GPS site velocities in the Tibetan Plateau and its vicinity. Shen et al. (2005) used a detailed GPS velocity field for the southeast borderland of the Tibetan Plateau to show that the crust is fragmented into tectonic blocks of various sizes. They also detected a new deformation zone, the Longriba fault, located ~150 km northwest of and in parallel with the Longmen Shan fault, with 4–6 mm/year right-slip rate.

The latest GPS data for the Tibetan Plateau are reported by Gan et al. (2007). The dataset includes 726 GPS stations; they cover the entire Tibetan Plateau and were surveyed in 1999, 2001, and 2004. These GPS data show that the rigid rotational component of crust within the Tibetan Plateau accommodates at least 50% of India's penetration into Eurasia. We use this latest dataset to constrain our model.

2.2. Three-dimensional elastic block models for the Tibetan Plateau

Most GPS site velocities, measured over a period of a few years, reflect mainly the interseismic crustal motion. Savage and Burford (1973) developed a one-dimensional (1-D) elastic dislocation model that associates the interseismic surface displacement rate with the long-term slip rate. This model has a straight, infinitely long strike-slip fault between two blocks in infinite elastic quarter-space. Between earthquakes, the fault is assumed to be locked to a constant depth, while below this depth the crust moves across this fault at the long-term, geologic slip rate. The station velocity is express as:

$$b = (v/\pi)\arctan(x/D) \tag{1}$$

Where, b is station velocity, v is the long-term fault slip rate, D is the locking depth, and x is distance from the fault.

To relate the GPS-measured interseismic crustal motion to the total slip rates (including both co- and interseismic slips) averaged over seismic cycles on multiple faults in a region, Meade et al. (2002) developed a three-dimensional elastic block model. The interseismic velocity is assumed to be the difference between block velocity and the yearly coseismic slip deficit (CSD) velocity:

$$\vec{v}_I = \vec{v}_B(\vec{x}_S) - \vec{v}_{CSD}(\vec{x}_S, \vec{x}_F) \tag{2}$$

Where, $\vec{x}_S$ is the station coordinate, and $\vec{x}_F$ represents the fault geometry. The block velocity is established using the rotation about an Euler pole:

$$\vec{v}_B(\vec{x}_S) = \Omega \times \vec{x}_S \tag{3}$$

The yearly coseismic slip deficit is calculated using a classic elastic dislocation model (Okada, 1985).

The block model provides a self-consistent field of the averaged "total" fault slip rates for a region of networked faults that can be constrained by GPS data. The predicted interseismic velocity at a point is equal to the sum of the block rotation rate and the integrated effects of elastic strain accumulation from all faults. The slip rates predicted by the block model are internally consistent in the sense that any closed path integral of velocity sums to zero (Meade et al., 2002; Meade and Hager, 2005a).

We used the same approach to construct a block model for eastern Tibet. The model is similar to that of Meade (2007), but with more details on the Songpan-Ganze region and using the latest GPS data (Gan et al., 2007). To limit the influence of artificial boundary conditions, our model includes much of the Tibetan Plateau. To minimize potential bias due to the GPS data, we eliminate all velocities with uncertainties large than 2.0 mm/year in their east or north component. The number of GPS station velocities used in our block model is 621.

We divided the fault-bounded blocks based on neotectonic and geodetic results of crustal motion in the region (Avouac and Tapponnier, 1993; Deng et al., 2002; Meade, 2007; Shen et al., 2005; Tapponnier et al., 2001; Zhang et al., 2003). The major faults in our model include the Himalayan Thrust System, the Sagaing fault, the Karakorum-Jiali fault, the east Kunlun fault, the Altyn Tagh fault, the Xianshuihe-Xiaojiang fault, and the Longmen Shan fault (Fig. 2). The Songpan-Ganze block is divided into three sub-blocks by the active

Please cite this article as: Wang, H., et al., Balance of seismic moment in the Songpan-Ganze region, eastern Tibet: Implications for the 2008 Great Wenchuan earthquake, Tectonophysics (2009), doi:10.1016/j.tecto.2009.09.022

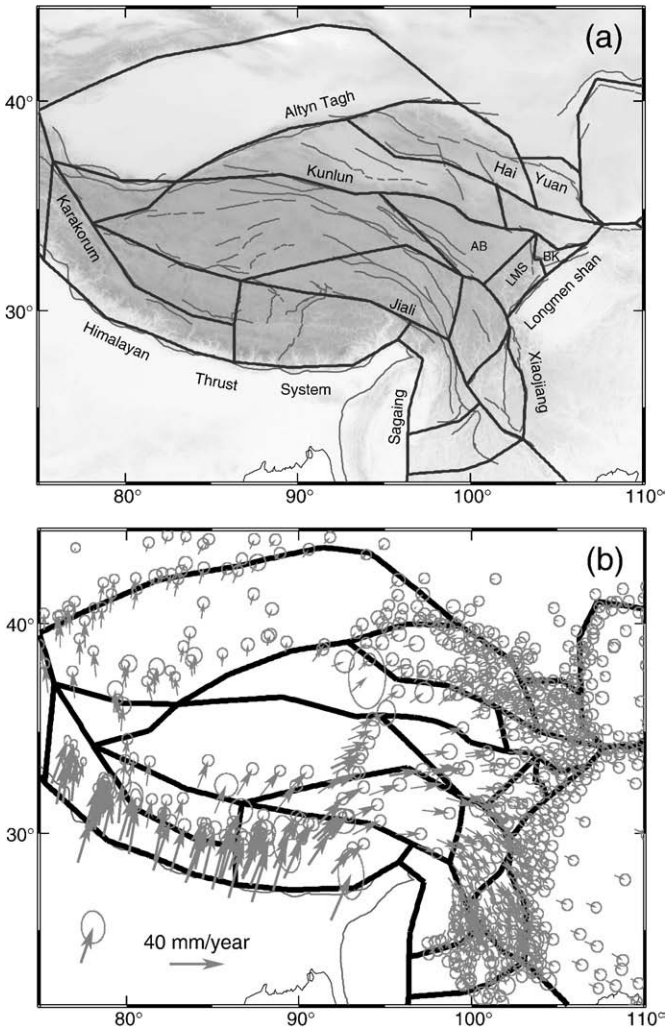

Fig. 2. (a) Block boundaries (black lines) of the block model of the Tibet Plateau. Gray lines are the major faults. (b) GPS velocities by Gan et al. (2007). AB, Aba sub-block; BK, Bikou sub-block; LMS, Longmen Shan sub-block.

faults: the Aba sub-block, the Longmen Shan sub-block, and the Bikou sub-block. The boundary between the Aba and the Longmen Shan sub-blocks is the Longriba fault (Shen et al., 2005; Xu et al., 2008). The boundary between the Longmen Shan and the Bikou sub-blocks is the Min Shan fault, which connects the eastern Kunlun fault and the Longmen Shan fault zone. To simplify the block model, the faults are assumed to be vertical with the exception of the Himalayan Thrust System, which dips ~10° northward, and the Longmen Shan fault zone, which dips 30° to the west (Ji, 2008; Wang et al., 2003).

2.3. Results of the elastic block model

One important parameter in the elastic block models is the locking depth of faults. A deeper locking depth would lead to broader strain distribution (Savage and Burford, 1973). Hence we need to determine the locking depths of the major faults.

Earthquake focal depth may be used to constrain the locking depth of faults. The hypocenter depths of the 1997 Manyi earthquake (Mw 7.6) and the 2001 Kokoxili earthquake (Mw 7.8) indicate that the locking depth of the Kunlun fault is about 15–20 km (Antolik et al., 2004; Peltzer et al., 1999). Results from earthquake relocation show that about 77% of events in east Tibet occurred in the depth range of 0–15 km (Yang et al., 2005). We started with a 15 km locking depth for all faults in eastern Tibet and then iterated for the optimal locking depths for the Xianshuihe fault and the Longmen Shan fault. Fig. 3 shows how the model fits the geodetic data for a range of locking depths for the Xianshuihe and the Longmen Shan faults. The optimal locking depth is obtained through the chi-square test: $\chi^2 = r^T C^{-1} r$, where r is the vector of residual velocities and C is the data covariance matrix (Meade et al., 2002). The best fit is obtained with 17 km locking depth for the Xianshihe fault and 20 km for the Longmen Shan fault. These results are consistent with previous studies (Ji, 2008; Wang et al., 2007; Yang et al., 2005).

Using the optimal locking depths for the major faults, we inverted slip rates on these faults in the three-dimensional block model. The model predictions are in good agreement with the GPS velocity field (Fig. 4). The misfits of velocity are mainly found around the southern boundary of the Tibetan Plateau, where the GPS stations are sparse and observational errors are large. The mean residual velocity is 1.09 mm/year, less than the 2–3 mm/year uncertainty of the GPS data with 90% confidence (Gan et al., 2007). About 73% of the residual velocity components are smaller than the 1-σ uncertainty of the GPS data (1.44 mm/year).

Fig. 5 shows the predicted slip rates. Similar to previous studies, we found the most active faults in the Tibetan Plateau to be the plate boundary faults: the Himalayan thrust system and the India–Sundaland fault system. The right-lateral slip rate on the India–Sundaland boundary fault system is about 35.1 ± 1.1 mm/year, comparable with

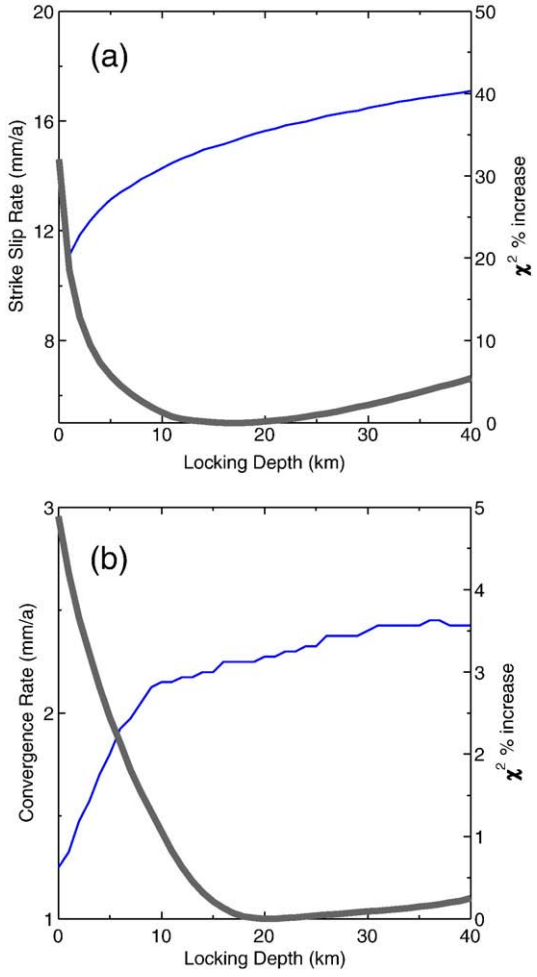

Fig. 3. "(a) Fit to data (right axis and gray line) and slip rate (left axis and blue line) on the Xianshuihe fault as a function of their locking depth; (b) Fit to data (right axis) and slip rate (left axis) on the Longmen Shan fault. (For interpretation of the references to color in this figure legend, the reader is referred to the web version of this article.)

Please cite this article as: Wang, H., et al., Balance of seismic moment in the Songpan-Ganze region, eastern Tibet: Implications for the 2008 Great Wenchuan earthquake, Tectonophysics (2009), doi:10.1016/j.tecto.2009.09.022

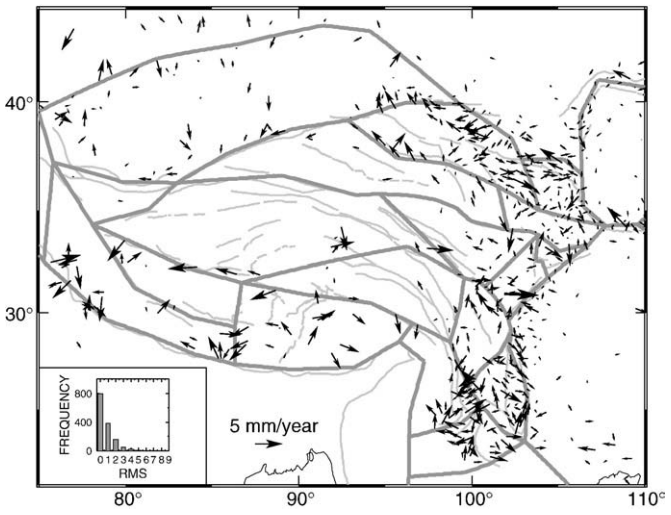

Fig. 4. Residual velocities (differences between the GPS velocities and model predictions) in the Tibetan Plateau. Thin lines are the major faults; thick lines show the geometry of the block model. The inset shows the distribution of root mean square (RMS) residual velocities (in mm/year).

previous results (Vigny et al., 2003). The dip-slip along the Himalayan thrust system is about 14.6 ± 1.3 mm/year, less than Meade's result (Meade, 2007) but consistent with other studies (Shen et al., 2000; Wang et al., 2001; Zhang et al., 2004).

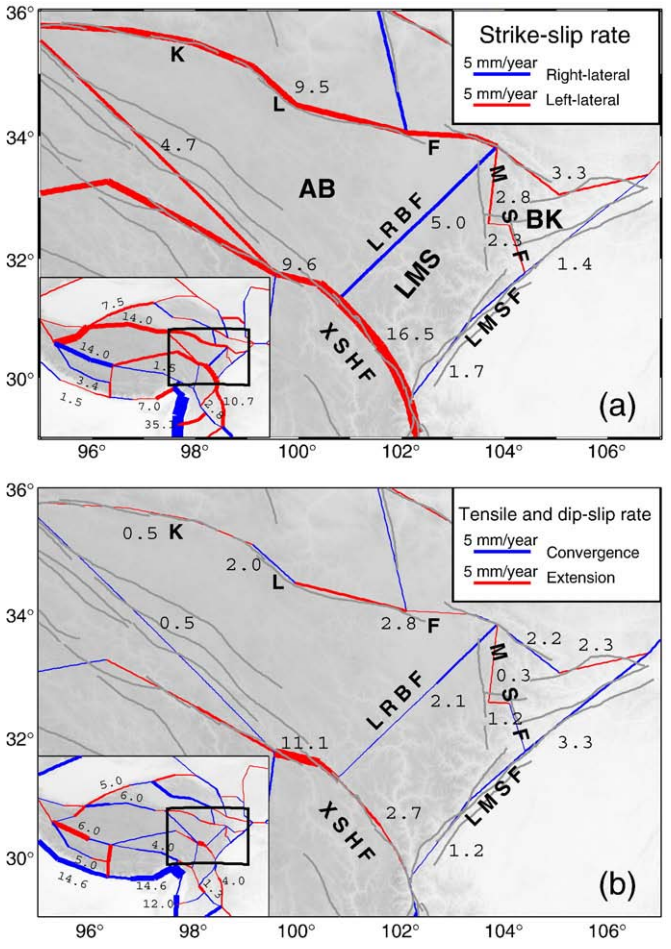

Fig. 5. The predicted strike-slip rate and dip-slip rate on major faults in the Songpan-Ganze region. KLF, eastern Kunlun fault; MSF, Minshan fault; LMSF, Longmen Shan fault; LRBF, Longriba fault; XSHF, Xianshuihe fault; AB, Aba block; BK, Bikou block; LMS, Longmen Shan block. Insets show the results of the regional model and the location of the Songpan-Ganze region.

The east–west striking faults across the Tibetan Plateau are mainly strike-slip faults. Along the Xianshuihe fault, the predicted left-lateral slip rate is 9.6 ± 1.3 mm/year on the northwestern segment and 16.5 ± 0.8 mm/year on the southeastern segment. These results are consistent with previous results (Allen et al., 1991; Shen et al., 2005; Wang et al., 1998; Wang et al., 2008b). The slip rates are 14.9 ± 1.1 mm/year on the western segment of the eastern Kunlun fault, and 3.3 ± 1.5 mm/year near the eastern ends of the eastern Kunlun fault, consistent with previous studies (Kirby et al., 2007; Lin and Guo, 2008; Woerd et al., 2000). The left-lateral slip rates on the Altyn Tagh fault range from 1.3 ± 0.4 mm/year to 7.9 ± 0.6 mm/year and show westward increase. The results are comparable with others results (Bendick et al., 2000; Zhang et al., 2007).

South–north shortening occurs in the entire Tibetan Plateau. The shortening rate across north Tibetan Plateau is about 10.5 ± 1.2 mm/year. The western segment of the eastern Kunlun fault also absorbs 6.0 mm/year convergence. The north-striking faults in the central part of the southern Tibetan Plateau are extensional with 10 mm/year dip-slip. This is consistent with the eastward-extruding of the Tibetan crust (Blisniuk et al., 2001; Chen et al., 2004; Kapp et al., 2008; Liu and Yang, 2003; Royden et al., 2008).

The northeast-trending faults in eastern Tibet are mainly reverse faults. Along the Longmen Shan fault, the convergence rate is 1.2 ± 1.0 mm/year along the southwestern segments and 3.3 ± 1.3 mm/year on the northeastern segments. These low slip rates are comparable with previous estimates (Burchfiel et al., 2008; Chen et al., 2000; Densmore et al., 2007; King et al., 1997; Shen et al., 2005; Zhang et al., 2004). There is also a right-lateral strike-slip motion on the Longmen Shan fault zone: 1.7 ± 0.7 mm/year along the southwestern segments and 1.4 ± 1.1 mm/year on the northeastern segments. On the Longriba fault, the right-lateral strike-slip is 5.0 ± 1.2 mm/year and the convergence rate is 2.1 ± 1.2 mm/year, at the same level with those on the Longmen Shan fault (Wang et al., 2008b).

2.4. Predicted moment accumulation rates in the Songpan-Ganze region

Using the predicted fault slip rates, we calculated the accumulation rate of seismic moments (M_o) on each fault segment: $M_o = \sum \mu |s| A$ where s is the slip rate of the fault segment, A is the area of locked fault plane, and μ is the shear modulus. Using a shear modulus of $\mu = 30$ GPa and the optimal locking depths, we found that the moment accumulates at $1.24 \pm 0.17 \times 10^{20}$ N m/year for the entire Tibetan Plateau, slightly less than the 1.65×10^{20} N m/year in Meade's model (Meade, 2007). The different results may be attributed to the different geometry of blocks in these models.

The moment accumulation rates are directly related to the fault slip rates. The eastern Kunlun fault accumulates at $1.73 \pm 0.22 \times 10^{19}$ N m/year, or 14% of the total moment accumulation rate in the plateau. The Xianshuihe-Xiaojiang fault accumulates at $7.19 \pm 0.63 \times 10^{18}$ N m/year, about 5% of total moment accumulation in the Tibetan Plateau. Fig. 6 shows the predicted accumulation rates in the Songpan-Ganze region, the focus of this study. The total moment accumulation in this region is $1.08 \pm 0.25 \times 10^{19}$ N m/year. The highest moment accumulation rate is on the eastern Kunlun fault, about $3.14 \pm 0.17 \times 10^{18}$ N m/year. Moment accumulation rate is about $2.35 \pm 0.16 \times 10^{18}$ N m/year on the Xianshuihe fault, but only $1.06 \pm 0.35 \times 10^{18}$ N m/year on the Longmen Shan fault because of the low slip rates.

Assuming the moment accumulation rates are constant through late Quaternary (Chen et al., 2000; King et al., 1997; Royden et al., 2008), the accumulated moment in the entire Songpan-Ganze region over 150 years is barely sufficient for an Ms 8.0 earthquake, and this is assuming all the moment would be released by earthquakes. Yet two M ≥ 8.0 and several M ≥ 7.0 earthquakes occurred in the Songpan-Ganze region during the last 100 years. Hence we need to examine a longer history of seismic moment evolution.

Please cite this article as: Wang, H., et al., Balance of seismic moment in the Songpan-Ganze region, eastern Tibet: Implications for the 2008 Great Wenchuan earthquake, Tectonophysics (2009), doi:10.1016/j.tecto.2009.09.022

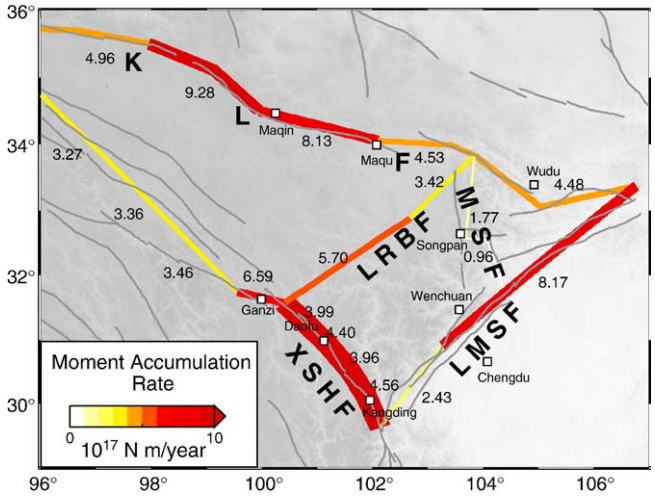

Fig. 6. Scalar moment accumulation rate in the Songpan-Ganze region. Abbreviations are explained in Fig. 5. Numbers are in 10^{17} N m/year for various segments of the faults.

3. Seismicity and moment release in the Songpan-Ganze region

In this section, we examine seismicity and the release of seismic moment in the Songpan-Ganze region. By comparing the seismic moment release with the predicted seismic moment accumulation, we hope to gain some insights into the occurrence of the 2008 Great Wenchuan earthquake and earthquake hazards in the Songpan-Ganze region.

3.1. Seismic activity in the Songpan-Ganze region

Seismic activity in the Songpan-Ganze region is intense (Fig. 1). Most earthquakes occur on the eastern Kunlun-Bailong Jiang fault, the Longmen Shan-Min Shan fault, and the Xianshuihe fault. Many large earthquakes were recorded in these faults since 1900, including the M 7.2 Luhuo-Daofu earthquake in 1923, the M 7.5 Diexi earthquake in 1933, the M 7.5 Tuosuo Lake earthquake in 1937, the M 7.5 Kangding earthquake in 1955, the M 7.0 Alake lake earthquake in 1963, the M 7.6 Luhuo earthquake in 1973, and the Songpan earthquakes in 1976 (Chen et al., 1994; Division of Earthquake Monitoring and Prediction, C.S.B, 1999; Guo et al., 2007; Wen et al., 2008) (Table 1). The spatial-temporal distribution of these historical earthquakes is uneven, making it necessary to analyze seismic activity on each fault zone.

The eastern Kunlun fault has higher rates of fault slip and seismic moment accumulation (Figs. 5 and 6). However, because of the high altitude and sparse population, no historic earthquake was recorded before 1900. Two major events occurred since then: the M 7.5 Tuosuo lake earthquake in 1937, and the M 7.0 Alake lake earthquake in 1963. The first event had a ~150 km long surface rupture with 4.1 m mean left-lateral offset (Guo et al., 2007). The source parameters of the 1963 Alake lake earthquake were recorded by several instruments at that time (Molnar and Lyon-caen, 1989). Surface rupture is estimated to be ~40 km long, with 1–2 m left-lateral slip (Guo et al., 2007). Although there is no record of historical earthquakes on the Maqin–Maqu segments of the Kunlun fault (Fig. 1), field investigation found a surficial rupture along the western section of Maqu; the age of the rupture is thought to be during the last half of the 19th century (Wen et al., 2007). The eastern end of the Kunlun fault is marked by the M 8.0 Wudu earthquake in 1879 (Fig. 1) (Division of Earthquake Monitoring and Prediction, S.S.B, 1995). Although the source parameters of this event are unknown, the extreme earthquake damage and surface ruptures have been well documented (Hou et al., 2005).

The Xianshuihe fault is marked by clusters of earthquakes, separated by periods of relative quiescence. Seismic activity was intense from 1700 to 1817, quiescent from 1818 to 1892, and active again since 1893, with five M≥7.0 events: the M 7.2 Daofu earthquake in 1893, M 7.0 Daofu earthquake in 1904, the M 7.2 Daofu earthquake in 1923, and the M 7.5 Kangding earthquake in 1955, and the M 7.6 Luhuo earthquake in 1973. The source parameters of these earthquakes were established by field investigation and instruments (Allen et al., 1991; Papadimitriou et al., 2004; Wen et al., 2008). After the Daofu earthquake (M 6.9) in 1981, no M≥6.0 events have occurred on this part of the Xianshuihe fault.

On the Longmen Shan-Min Shan fault system, all major earthquakes occurred on the Min Shan fault, including the 1933 Diexi earthquake (Ms 7.5) and the 1976 Songpan earthquakes (Ms 7.2, 6.7, 7.2). The 1933 Diexi earthquake occurred on a fault plane trending 14° and dipping 60° to the southeast with right-lateral strike slip (Chen et al., 1994). Fault planes of the 1976 Songpan earthquakes show a combination of reverse and left-lateral strike-slip motion (Jones et al., 1984). There were three moderate events on the Longmen Shan fault: the Ms 6.5 Wenchuan earthquake in 1657, the Ms 6.2 Beichuan earthquake in 1958, and the Ms 6.2 Dayi earthquake in 1970 (Chen et al., 1994), all occurred on the middle and southwestern segments of the Longmen Shan fault. Seismicity on the northeastern segment of the Longmen Shan fault is low, and no M≥7.0 earthquakes were recorded on the entire Longmen Shan fault before the Great Wenchuan earthquake.

There were also several M≥6.0 earthquakes in the interior of the Songpan-Ganze region since 1900. Comparing with the main faults, seismicity in the interior of the Songpan-Ganze region is low. The

Table 1
Earthquakes of M≥6.0 in the Songpan-Ganze region since 1879.

Event	Date	Magnitude (Ms)	Epicenter		Location[a]
			Longitude	Latitude	
1	1879-07-01	8.0	104.7	33.2	South of Wudu (1)
2	1881-07-20	6.5	104.6	33.6	Lixian (1)
3	1893-08-29	7.2	101.5	30.6	Daofu (3)
4	1904-08-30	7.0	101.1	31.0	Daofu (3)
5	1919-05-29	6.3	100.5	31.5	Daofu (3)
6	1919-08-26	6.2	100.0	32.0	Ganze (3)
7	1923-03-24	7.2	100.8	31.3	Daofu (3)
8	1930-04-28	6.0	100.0	32.0	Ganze (3)
9	1932-03-07	6.0	101.8	30.1	Kangding (3)
10	1933-08-25	7.5	103.7	32.0	Diexi (2)
11	1935-07-26	6.0	101.1	33.3	Jiuzi (4)
12	1937-01-07	7.5	97.6	35.5	Tuosuo (1)
13	1938-03-14	6.0	103.6	32.3	South of Songpan (2)
14	1941-06-12	6.0	102.5	30.1	Luding (2)
15	1941-10-08	6.0	102.3	31.7	Heishui (4)
16	1947-03-17	7.7	99.5	33.3	Dari (4)
17	1949-06-15	6.0	100.0	33.3	Banma (4)
18	1952-11-01	6.0	101.0	33.3	Jiuzi (4)
19	1955-04-14	7.5	101.9	30.0	Kangding (3)
20	1958-02-08	6.2	104.3	31.7	Beichuan (2)
21	1960-11-09	6.8	103.66	32.78	Zhangla (2)
22	1963-04-19	7.0	97.0	35.7	Alake(1)
23	1967-08-30	6.8	100.3	31.6	Luhuo (3)
24	1967-08-30	6.6	100.23	31.63	Luhuo (3)
25	1970-02-24	6.2	103.2	30.6	Dayi (2)
26	1971-03-24	6.3	98.1	35.45	Tuosuo Lake (1)
27	1973-02-06	7.6	100.24	31.5	Luhuo (3)b
28	1973-02-08	6.0	100.5	31.6	Luhuo (3)
29	1973-08-11	6.5	103.9	32.93	Huanglong (2)
30	1976-08-16	7.2	104.13	32.61	Songpan (2)
31	1976-08-22	6.7	104.4	32.6	Songpan (2)
32	1976-08-23	7.2	104.3	32.5	Songpan (2)
33	1981-01-24	6.9	101.1	31.0	Daofu (3)
34	1982-06-16	6.0	99.75	31.86	Ganze (3)
35	1989-09-22	6.5	102.51	31.58	North of Xiaojin (4)
36	1995-12-18	6.2	97.3	34.6	Guoluo (4)

[a] Earthquake locations: (1) earthquake associated with the eastern Kunlun fault, (2) earthquakes related to the Longmen Shan-Min Shan fault zone, (3) earthquakes on the Xianshuihe fault zone, (4) earthquake that occurred outside the eastern Kunlun fault, Longmen Shan-Min Shan and Xianshuihe faults (data from Chen et al., 1994; Division of Earthquake Monitoring and Prediction, S.S.B, 1995, 1999).

largest event was an M 7.7 earthquake in the eastern Tibetan Plateau in 1947. The seismic parameters for these events are unclear.

3.2. Relationship between surface magnitude (Ms) and scalar moment (Mo) in the Tibetan Plateau

A complete record of earthquakes is essential for accurately estimating the seismic moment release. Fig. 7 shows that historical earthquakes recorded in the Songpan-Ganze region are mainly after 1879. Clearly, smaller earthquakes are more likely to be missed in the catalog. Previous analyses have suggested that, in the Songpan-Ganze region, records for events of magnitude greater than 6.0 are likely complete since 1879 (Huang et al., 1994; Qin et al., 1999).

Most earthquakes in the Chinese catalog are given in surface-wave magnitude (Ms), whereas the scalar moment (Mo) is usually given by the moment magnitude (Hanks and Kanamori, 1979):

$$M_w = (2/3)\log M_o - 6.03 \quad (4)$$

with M_o in Newton-meter. Because of the different empirical formulae and observational instruments used in China, the magnitude in Chinese earthquake catalog differs from that in the US earthquake catalog for the same event (Liu et al., 2006). Hence we need to calibrate the relationship between regional surface-wave magnitude (Ms) and scalar moment.

The Harvard centroid moment catalog (now the Global CMT catalog) provides scalar moment for global earthquake with magnitude > 5.5 since 1976. We use this catalog to calibrate the relationship between surface-wave magnitude and scalar moment in the Tibetan Plateau. We select the earthquakes occurred in and around the Tibetan Plateau that are listed in the Harvard catalog, and compare the scalar moment with the surface magnitude in the Chinese earthquake catalog. We select only $M \geq 6.0$ events. The relationship between surface magnitudes of the Chinese catalog with scalar moments (in N m) is established by least-squares fitting:

$$\text{Log } M_o = 7.5967(\pm 0.8049) + 1.6073(\pm 0.1243) M_s \quad (5)$$

The correlation coefficient is 0.8377 (Fig. 8).

3.3. Seismic moment release in the Songpan-Ganze region

Using Eq. (5), we estimated the scalar moment released by earthquakes in the Songpan-Ganze region based on the Chinese historical and instrumental earthquake record. The total seismic moment released is $8.70 \pm 5.48 \times 10^{20}$ N m in the Songpan-Ganze region during 1879–2007, assuming the error of surface-wave magnitude in the Chinese earthquake catalog is ±0.2. This is because the Ms in the Chinese catalog is generally 0.2 higher than that in the U.S. catalog (Liu et al., 2006).

The moment release is unevenly distributed in the Songpan-Ganze region (Fig. 9). With high slip rates and frequent large earthquakes, the Xianshuihe fault has released 28.57×10^{19} N m since 1879. Only five $M \geq 6.0$ historical earthquakes were recorded on the eastern Kunlun fault since 1879. The moment release concentrated on the Tuosuo Lake segment (5.29×10^{19} N m) and the Bailong fault

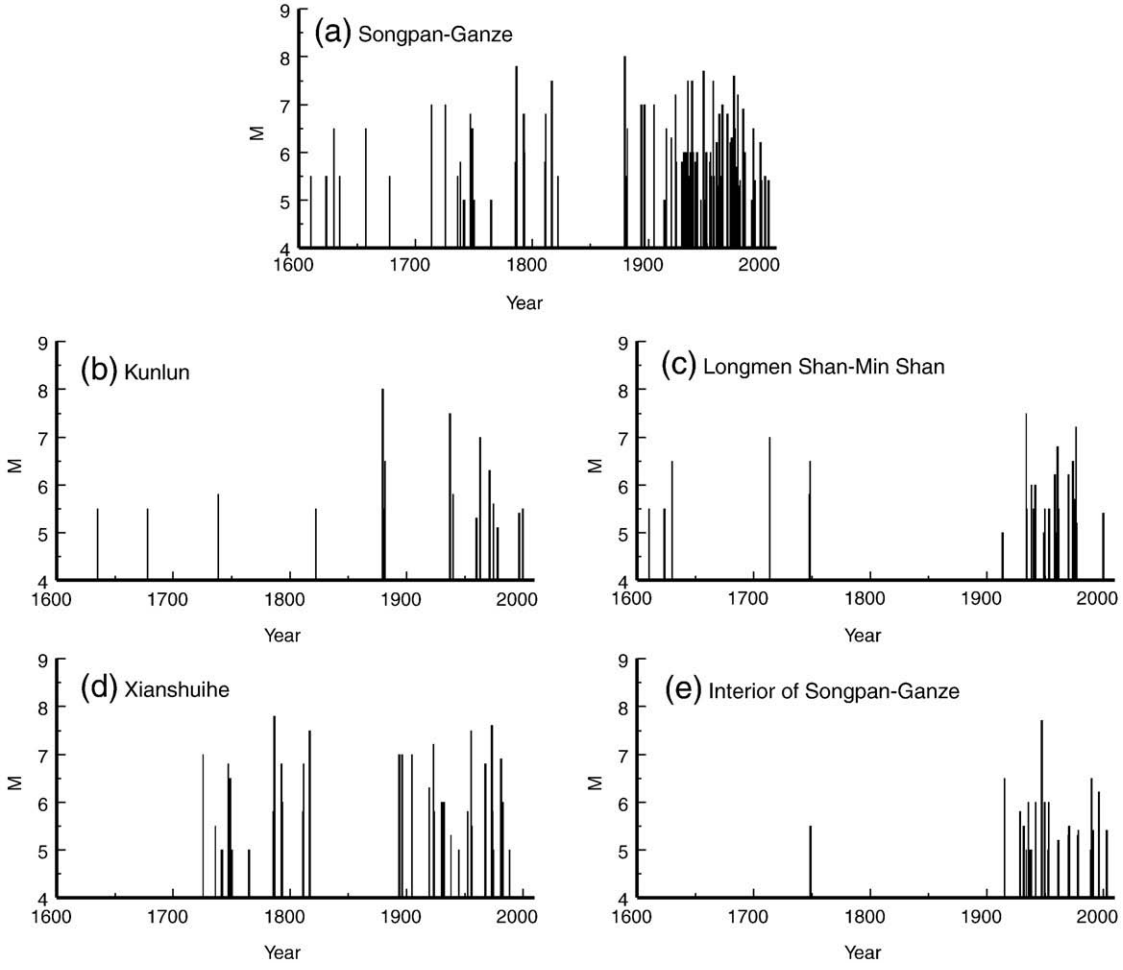

Fig. 7. Magnitude–time plot of historical and instrument-recorded earthquakes in the Songpan-Ganze region (a) and the major faults (b–e). Data sources: Chen et al. (1994), Division of Earthquake Monitoring and Prediction, S.S.B (1995, 1999).

Please cite this article as: Wang, H., et al., Balance of seismic moment in the Songpan-Ganze region, eastern Tibet: Implications for the 2008 Great Wenchuan earthquake, Tectonophysics (2009), doi:10.1016/j.tecto.2009.09.022

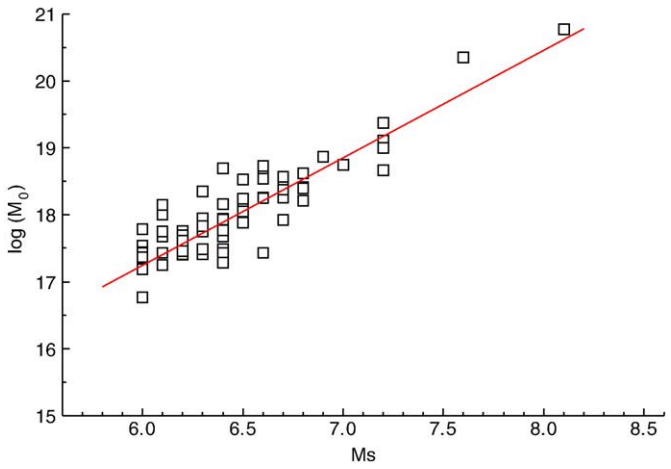

Fig. 8. Correlation of scalar moment (in N m) from the Global CMT catalog and the surface magnitude (Ms) in the Chinese earthquake catalog for selected earthquakes in the Tibetan Plateau and its vicinity.

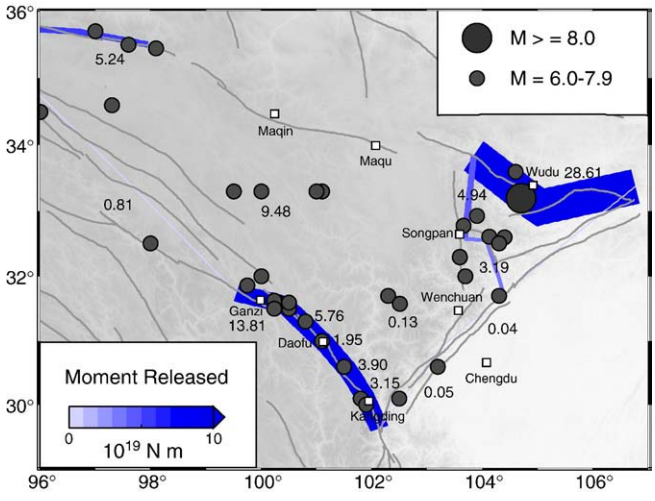

Fig. 9. Released seismic moment on the faults in the Songpan-Ganze region between 1879 and 2007. Line thickness is proportional to the scalar moment. Circles are the earthquakes included in the calculation. Numbers are in 10^{19} N m for various segments of the faults.

(28.60×10^{19} N m). The most moment release was by the M 8.0 Wudu earthquake in 1879 (Fig. 1). The complete historical earthquakes (for $M\geq6.0$ events) on the Longmen Shan-Min Shan fault can date back to 1600. The total scalar moment released is about 8.90×10^{19} N m since 1600, mostly by the series of Songpan earthquakes in 1976. The total seismic moment released on the Longmen Shan fault is only 0.09×10^{19} N m in the last 400 years (Table 2).

The recurrence intervals of major earthquakes in the Songpan-Ganze region are hundreds to thousands of years (Burchfiel et al., 2008; Guo et al., 2007; Lin and Guo, 2008; Van der Woerd et al., 2000; Van der Woerd et al., 2002; Wen et al., 2008), longer than the 400 years covered by the available earthquake catalog. Given the clustering of major earthquakes on those main faults (Yi et al., 2002), the rates of moment release between 1879 and 2007, a period of high seismicity, may be higher than the average moment release rate.

4. Moment deficits in the Songpan-Ganze region

Moment deficit is the seismic moment on a fault that is available to produce earthquakes (Meade and Hager, 2005b). Here we determine the moment deficit on major faults in the Songpan-Ganze region by comparing the predicted moment accumulation with that released by earthquakes. The moment deficit thus determined is the higher bound, because not all the predicted moment would be released by earthquakes.

4.1. Moment balance: 1879–2007

Because complete records of $M\geq6.0$ events in the Songpan-Ganze region may extend back to 1879 (Huang et al., 1994; Qin et al., 1999), we examine here the seismic moment accumulation and release between 1879 and 2007, before the 2008 Wenchuan earthquake.

The moment accumulation from 1879 to 2007 is about $1.39\pm0.31\times10^{21}$ N m for the entire Songpan-Ganze region, mostly on the southeastern Xianshuihe fault and the eastern Kunlun fault (Fig. 10a). Along the eastern Kunlun fault, the M 8.0 Wudu earthquake in 1879 released more moment than that accumulated from 1879 to 2007 (Fig. 10a), hence the easternmost segment of the Kunlun fault has a big moment surplus (i.e., overspent seismic moment) by 2007 (Fig. 10b). The Maqin–Maqu segments of the eastern Kunlun fault have large moment deficits during this period, enough to produce an Mw 7.3 event if all these segments rupture simultaneously.

On the Xianshuihe fault, fast moment accumulation is nearly balanced by fast moment release by earthquakes during this period. The M 7.6 Luhuo earthquake caused a moment surplus on the Ganze-Daofu segment. On the other segments of the Xianshuihe fault, moment accumulation is slightly more than moment release. The total moment deficit on the segments south of Daofu is about 7.54×10^{19} N m, barely enough for an Mw 7.0 event (Fig. 10b).

Several M 7.0 earthquakes on the Min Shan fault in the last century led to a moment surplus (Fig. 10b). In contrast, low moment release on the Longmen Shan fault led to moment deficits: 10.42×10^{19} N m

Table 2
Fault slip rate, predicted rate of moment accumulation, and seismically released moment on the selected faults in the Songpan-Ganze region.

Fault zone name	Fault slip rate			Moment accumulation rate (10^{17} N m/year)	Seismic moment release (10^{19} N m)
	Strike-slip rate (mm/year)	Tensile-slip rate (mm/year)	Dip-slip rate (mm/year)		
Eastern Kunlun					
Tuosuo Lake segment	9.5 ± 1.5	-0.7 ± 1.7	...	4.96	5.24
Maqin–Maqu segment	8.9 ± 1.2	-4.2 ± 1.0	...	8.13	...
Eastern end segment	3.3 ± 1.5	2.2 ± 1.3	...	4.48	28.61
Longmen Shan					
Northeastern segment	-1.4 ± 1.1	...	3.3 ± 1.1	8.17	0.04
Southwestern segment	-1.7 ± 0.9	...	1.2 ± 1.0	2.43	0.05
Min Shan	2.5 ± 1.5	0.8 ± 1.6	...	2.73	8.13
Xianshuihe	14.9 ± 0.9	-5.5 ± 1.2	...	23.50	28.57
Longriba	5.0 ± 1.2	2.1 ± 1.2	...	9.12	...

Positive and negative strike-slip rates give left- and right-lateral motion, respectively. Positive and negative dip-slip rates give thrust and normal motion, respectively. Positive and negative tensile-slip rates give closing and opening motion, respectively. In all cases, the slip rate is evaluated at the middle of the segment.

Please cite this article as: Wang, H., et al., Balance of seismic moment in the Songpan-Ganze region, eastern Tibet: Implications for the 2008 Great Wenchuan earthquake, Tectonophysics (2009), doi:10.1016/j.tecto.2009.09.022

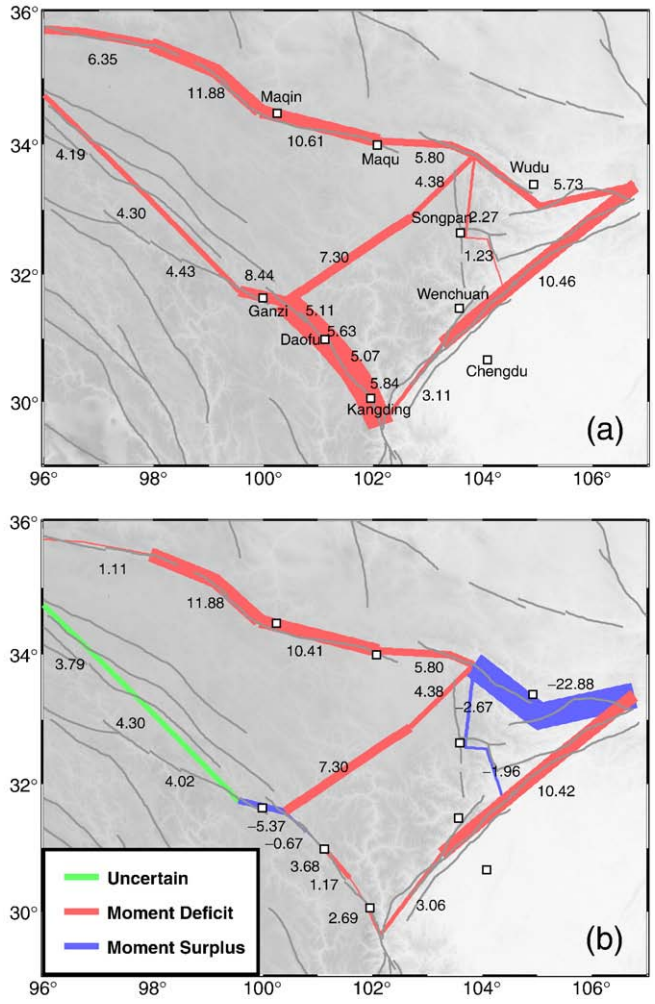

Fig. 10. (a) Scalar moment accumulation from 1879 to 2007; (b) moment balance for the period of 1879–2007. Positive values are "moment deficit" — moment that has not been released by earthquakes. Line thickness is proportional to the scalar moment. (in 10^{19} N m/year).

on the central-northern segment and 3.06×10^{19} N m on the southern segment.

4.2. Moment deficits in the past millennium

Over the seismic cycles, seismic moment on a fault trends to be balanced. The large moment deficit and surplus in Fig. 10b indicate that the period we examined, from 1879 to 2007, is too short in comparison with the recurrence intervals of $M\geq6.0$ earthquakes on these faults, except perhaps on the southeastern Xianshuihe fault where moment is nearly balanced. Paleoseismological and neotectonic studies suggest that the upper-bound of the recurrence interval of large earthquakes on the eastern Kunlun fault is about 400–760 years (Guo et al., 2007; Van der Woerd et al., 2000; Van der Woerd et al., 2002). The recurrence interval for a M 7.0 earthquake is about 100–200 years on the Xianshuihe fault (Kato et al., 2007; Wen et al., 2008), and hundreds of years for the Min Shan fault (Zhang et al., 2005).

From 1879 to 2007, the accumulated moment deficit on the central-northern Longmen Shan fault is 10.42×10^{19} N m, barely enough for a Mw 7.3 event. Clearly, the moment released by the 2008 Wenchuan earthquake had been accumulating for a much longer time. The earliest earthquake recorded on the Longmen Shan fault zone was a M 5.5 event on Sept. 15, 1488 (Chen et al., 1994). An M 6.5 event occurred near Wenchuan on April 21, 1657. No earthquake greater than M 6.0 is likely missed in the record since then. Balancing moment for the period of 1657–2007 indicates a 37.0×10^{19} N m deficit on the Longmen Shan fault, still insufficient for an M 8.0 earthquake. Hence the recurrence intervals of large earthquakes on the Longmen Shan fault are even longer (Burchfiel et al., 2008; Densmore et al., 2007; Zhang et al., 2008). Field studies indicate that the last large earthquake on the Beichuan fault, part of the ruptured central Longmen Shan fault system, occurred at least 1000 years ago (Densmore et al., 2007). Fluvial terraces on the Yingxiu-Beichuan and Guanxian-Jiangyou faults are dated to 3000–10,000 years ago, and have not been offset by earthquakes since their formation (Zhou et al., 2007).

Assuming no large earthquakes, except those moderate events in the catalog, have occurred on the Longmen Shan fault in the past 1000 years, and assuming the moment was balanced about 1000 years ago, we estimated the moment deficit that would be expected by 2007 (Fig. 11a). The moment deficit on the central-northern Longmen Shan segment would be close to 113.9×10^{19} N m, enough to produce the 2008 Great Wenchuan earthquake.

For the eastern Kunlun fault and the southeastern Xianshuihe fault, 1000 years would include a few seismic cycles. We calculate only the deficit since 1600, assuming the moment was balanced before 1600. The results show much lower moment deficit on these faults in comparison with the Longmen Shan fault (Fig. 11a). The moment deficit and the implied earthquake risks derived from such analysis are in contrast to the high earthquake risks on the

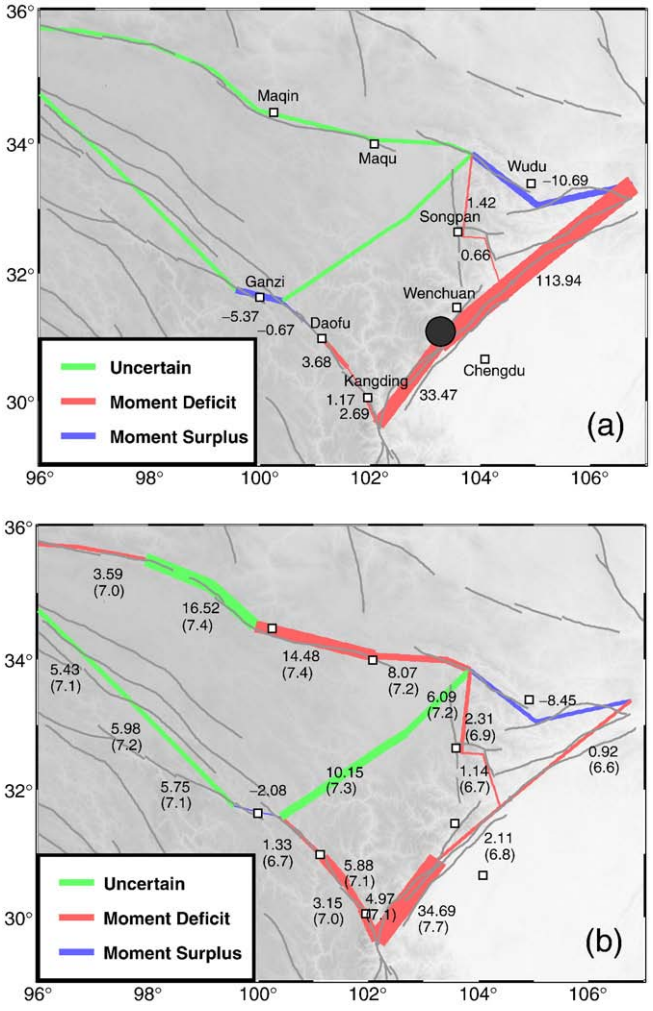

Fig. 11. (a) Estimated regional moment balance before 2008 in the past millennium. (b) Predicted moment balance 50 years from today. Numbers in brackets indicate the moment magnitude of potential earthquakes, if all the moment deficits are released seismically in a single rupture. Line thickness is proportional to the scalar moment. (in 10^{19}N m/year).

Please cite this article as: Wang, H., et al., Balance of seismic moment in the Songpan-Ganze region, eastern Tibet: Implications for the 2008 Great Wenchuan earthquake, Tectonophysics (2009), doi:10.1016/j.tecto.2009.09.022

southeastern Xianshuihe fault and low risks on the Longmen Shan fault inferred from the recorded historic earthquakes alone.

4.3. Moment deficit in another 50 years

Following the analysis outlined above, we attempted to predict the moment deficit for the next 50 years (Fig. 11b). We focus on the eastern part of the Songpan-Ganze region, where earthquake records are more complete. The results in Fig. 11b is derived by 1) using the same assumptions for deriving the results in Fig. 11a, 2) including 1.15×10^{21} N m released by the 2008 Great Wenchuan earthquake, and 3) assuming no large earthquakes in the next 50 years. The moment deficit will be low on the central-northeastern segments of the Longmen Shan fault because of the 2008 Wenchuan earthquake, hence a repeat of a large earthquake on this segment of the Longmen Shan fault is unlikely in the next 50 years or even longer. The largest moment deficit will be on the southwestern segment of the Longmen Shan fault. If all the moment is released by a rupture of the whole segment, it could produce an earthquake as large as Mw 7.7 in the next 50 years.

Other high risk fault segments include the Maqin–Maqu segment of the eastern Kunlun fault, where the slip rates are high and seismicity has been quiescent for the past 100 years (Wen et al., 2007). These segments of the Kunlun fault could produce an Mw 7.4 event in the next 50 years. On the Xianshuihe fault, the largest potential earthquake in the next 50 years would be an Mw 7.1 event along the Daofu-Kangding segment.

These results differ from that implied by recent studies of Coulomb stress changes associated with the 2008 Wenchuan earthquake (Parsons et al., 2008; Toda et al., 2008), because these studies do not consider influence from previous earthquakes. Luo and Liu (2009-this volume) reached similar conclusions as ours by including historic earthquakes in their geodynamic model of Coulomb stress evolution.

5. Discussion

We have used the elastic block model to calculate slip rates on the major fault zones in the Songpan-Ganze region. This model assumes crustal deformation concentrating along fault zones bounding rigid crustal blocks (Meade and Hager, 2005a), although some authors have argued that crustal deformation in the Tibetan Plateau is continuously distributed (England and Molnar, 2005; Zhang et al., 2004). Recent studies have shown that the block model is well suited to describe short-term deformation within the Tibetan Plateau (Meade, 2007; Thatcher, 2007).

When using GPS data to constrain the block model, one assumes that the GPS data represent interseismic deformation (Meade and Hager, 2005a). It is possible that some of the GPS data are tainted by postseismic deformation. However, for the large-scale model presented here, the influence of postseismic deformation is likely minor. The GPS data used here are from measurements in 1999, 2001, and 2004. The GPS data processing (Gan et al., 2007) attempted to remove coseismic displacements of the 2001 Mw 7.8 earthquake on the eastern Kunlun fault. The mean residual between the predicted and GPS velocities has the normal distribution, and is less than the ~3 mm/year uncertainties of the GPS data, so our elastic block model is not affected by postseismic deformation.

The uncertainties of our block model are largely due to the lack of GPS data in the central and southern Tibetan Plateau, where the residual velocities are up to 5 mm/year (Fig. 4). Consequently, the maximum errors of fault slips in these regions reach 4 mm/year. However, our focus is on the eastern Tibetan Plateau, where the GPS constraints are better than other parts of the plateau.

To balance seismic moment, we have to assume constant slip rates over the length of the earthquake catalog, and that the effects of distributed dissipative processes are negligible. The earthquake catalog should also be sufficiently long (Meade and Hager, 2005b; Swafford and Stein, 2007). Although the GPS survey represents the present-day crustal deformation, the GPS-indicated deformation pattern in the Tibetan Plateau is consistent with that inferred from Quaternary crustal deformation (King et al., 1997; Royden et al., 2008). Furthermore, the predicted slip rates are comparable with the geological slip rates. Hence the assumption of constant slip rates is reasonable.

Although a fault creep could release some seismic moment, and therefore affect the moment balancing, the effects of the creeping fault in eastern Tibet is likely minor. Creep along the Xianshuihe fault is less than 1.0 mm/year (Ran and He, 2006), and the creep-released moment is less than 5% of total moment accumulation on the Xianshuihe fault.

Another major parameter affecting the result of our model is the locking depth. Our estimated locking depth for the Xianshuihe fault is 17 km. This is consistent with the results of earthquake relocation (Wang et al., 2007; Yang et al., 2005). Using a 15 km locking depth for the Xianshuihe fault would reduce the predicted moment accumulation rate there by less than 4%.

The results of this study remind us once again the caveat of assessing earthquake hazards based on short and often incomplete catalog of historic earthquakes. The seismic hazard map (Zhang et al., 1999) of the Songpan-Ganze region feature a high seismic hazard along the Xianshuihe fault and the Min Shan fault; the Longmen Shan region is shown as a low risk region because of low seismic activity in the past century. However, the earthquake records on the Longmen Shan fault, dating back to 400 years ago, are nonetheless too short to reflect the seismicity of the fault, as paleoseismological data indicate a recurrence of large earthquakes in thousands of years (Densmore et al., 2007). In retrospect, the long-term seismic quiescence on the Longmen Shan fault before the 2008 Wenchuan earthquake should be regarded as a warning, and its seismic potential would be better assessed by taking into consideration the accumulated seismic moment as shown in our calculations (Fig. 11a).

6. Conclusions

We have calculated the fault slip rates of major faults in the Songpan-Ganze region and the rest of the Tibetan Plateau using a three-dimensional (3-D) elastic block model, constrained by the latest GPS data. We have used these slip rates to calculate the rates of seismic moment accumulation on the Longmen Shan and other major faults in the Songpan-Ganze region, and compared the results with seismic moment release estimated from earthquake catalogs. The major conclusions we may draw from this study include:

1) The slip rates for the eastern Kunlun fault and the Xianshuihe fault are much higher (up to 17 mm/year) than those for the Longmen Shan fault. The right-lateral and dip-slip rates on the Longmen Shan fault are 1.7 ± 0.8 mm/year and 1.2 ± 1.0 mm/year, respectively, along the southwestern segments, and 1.4 ± 1.1 mm/year and 3.3 ± 1.3 mm/year, respectively, on the northeastern segments.
2) The scalar seismic moment released in the Songpan-Ganze region is $8.70\pm5.48\times10^{20}$ N m from 1879 to 2007. The moment deficits over this period were concentrated on the western parts of the Xianshuihe and the eastern Kunlun faults. The series of large earthquakes on the eastern segment of the Xianshuihe fault has greatly reduced the moment deficit there. In the next 50 years, the largest event on the southeastern Xianhuihe fault is likely less than Mw 7.0.
3) Moment balance for the Longmen Shan fault over the past 400 years shows a moment deficit of 13.48×10^{19} N m, insufficient for the 2008 Great Wenchuan earthquake. From the moment balance, we conclude that no large earthquakes similar to the

Please cite this article as: Wang, H., et al., Balance of seismic moment in the Songpan-Ganze region, eastern Tibet: Implications for the 2008 Great Wenchuan earthquake, Tectonophysics (2009), doi:10.1016/j.tecto.2009.09.022

Great Wenchuan earthquake occurred on the Longmen Shan fault in the past 1400 years before May 12th, 2008. Similarity, a repeat of a major earthquake on the ruptured segment of the Longmen Shan fault is unlikely in the next 50 years.

4) In the next 50 years, all faults in the Songpan-Ganze region have moment deficits except the east end of the Kunlun fault. The largest moment deficits are on the southwestern segments of the Longmen Shan fault, capable of producing an Mw 7.7 event.

One major lesson we learned from this study is the caveat of earthquake hazard analysis based on short and incomplete earthquake records. For the Longmen Shan fault and many other active intraplate faults, the recurrence intervals of large earthquakes are thousands of years. On these faults, seismic quiescence in the past centuries should be treated with caution in earthquake hazards studies.

Acknowledgments

Wang's visit to the University of Missouri was supported by the NSF/PIRE grant 0730154 and MU matching fund to Liu, who also acknowledge support from the Chinese Academy of Sciences and the Ministry of Education of China for his research in China. This work is also supported by the Ministry of Science and Technology of China (Grant No. 2004CB418406), and the "Basic Science Research Plan" of the Institute of Earthquake Science, China Earthquake Administration (Grant No. 2007-03). We thank B. Meade for making his elastic block model available, and W. Gan for providing the latest GPS velocity data. This paper was improved by the constructive comments by guest editor J. Freymueller and two anonymous reviewers.

References

Allen, C.R., Luo, Z., Qian, H., Wen, X., 1991. Field study of a highly active fault zone: the Xianshuihe fault zone of southwestern China. Geological Society of America Bulletin 103, 1178–1199.

Antolik, M., Abercrombie, R.E., Ekstrom, G., 2004. The 14 November 2001 Kokoxili (Kunlunshan), Tibet, earthquake: rupture transfer through a large extensional step-ver. Bulletin of the Seismological Society of America 94 (4), 1173–1194.

Avouac, J.P., Tapponnier, P., 1993. Kinematic model of active deformation in central-Asia. Geophysical Research Letters 20 (10), 895–898.

Bendick, R., Bilham, R., Freymueller, J., Larson, K., Yin, G., 2000. Geodetic evidence for a low slip rate in the Altyn Tagh fault system. Nature 404 (6773), 69–72.

Blisniuk, P.M., et al., 2001. Normal faulting in central Tibet since at least 13.5 Myr ago. Nature 412, 628–632.

Burchfiel, B.C., Chen, Z., Liu, Y., Royden, L.H., 1995. Tectonics of the Longmen Shan and adjacent regions. International Geology Review 37, 661–735.

Burchfiel, B.C., et al., 2008. A geological and geophysical context for the Wenchuan earthquake of 12 May 2008, Sichuan, People's Republic of China. GSA Today 18 (7), 4–11. doi:10.1130/GSATG18A.1.

Chen, S., Wilson, C.J.L., Deng, Q., Zhao, X., Luo, Z., 1994. Active faulting and block movement associated with large earthquakes in the Min Shan and Longmen mountains, Northeastern Tibetan Plateau. Journal of Geophysical Research—Solid Earth 99 (B12), 24025–24038.

Chen, Z., et al., 2000. Global positioning system measurements from eastern Tibet and their implications for India/Eurasia intercontinental deformation. Journal of Geophysical Research—Solid Earth 105 (B7), 16215–16227.

Chen, Q.Z., et al., 2004. Spatially variable extension in southern Tibet based on GPS measurements. Journal of Geophysical Research—Solid Earth 109 (B9).

Deng, Q.D., et al., 2002. Basics characteristics of active tectonics of China (in Chinese). Science in China (Series D) 32 (12), 1020–1030.

Densmore, A.L., et al., 2007. Active tectonics of the Beichuan and Pengguan faults at the eastern margin of the Tibetan Plateau. Tectonics 26 (TC4005). doi:10.1029/2006TC001987.

Division of Earthquake Monitoring and Prediction, S.S.B, 1995. Catalog of Chinese Historical Strong Earthquakes (2300 BC–1911). China Seismological Press, Beijing.

Division of Earthquake Monitoring and Prediction, C.S.B, 1999. Catalog of Chinese historical strong earthquakes (1912–1990 Ms > 4.7). China Seismological Press, Beijing.

England, P., Molnar, P., 2005. Late Quaternary to decadal velocity fields in Asia. Journal of Geophysical Research—Solid Earth 110 (B12).

Gan, W., et al., 2007. Present-day crustal motion within the Tibetan Plateau inferred from GPS measurements. Journal of Geophysical Research—Solid Earth 112 (B08416). doi:10.1029/2005JB004120.

Guo, J., Lin, A., Sun, G., Zheng, J., 2007. Surface ruptures associated with the 1937 M 7.5 Tuosuo Lake and the 1963 M 7.0 Alake Lake earthquakes and the paleoseismicity along the Tuosuo Lake segment of the Kunlun Fault, Northern Tibet. Bulletin of the Seismological Society of America 97 (2), 474–496.

Hanks, T.C., Kanamori, H., 1979. A moment magnitude scale. Journal of Geophysical Research—Solid Earth 84 (B5), 2348–2350.

He, J., Liu, M., Li, Y., 2003. Is the Shanxi rift of northern China extending? Geophysical Research Letters 30 (232213).

Hou, K., Lei, Z., Wan, F., Li, L., Xiong, Z., 2005. Research on the 1879 southern Wudu M.0 earthquake and its coseismic rupture (in Chinese). Earthquake Research in China 21 (3), 295–310.

Huang, W.Q., Li, W.X., Cao, X.F., 1994. Research on the completeness of earthquake data in the Chinese mainland (II). Acta Seismologica Sinica 16 (4), 423–432.

Ji, C., 2008. Preliminary Result of the May 12, 2008 Mw 7.97 Sichuan Earthquake. http://www.geol.ucsb.edu/faculty/ji/big_earthquakes/2008/05/12/ShiChuan.html.

Jones, L.M., et al., 1984. Focal mechanisms and aftershock locations of the Songpan earthquakes of August 1976 in Sichuan, China. Journal of Geophysical Research—Solid Earth 89 (B9), 7697–7707.

Kapp, P., Taylor, M., Stockli, D., Ding, L., 2008. Development of active low-angle normal fault systems during orogenic collapse: insight from Tibet Geology, vol. 36, (1), pp. 7–10. doi:10.1130/G24054A.1.

Kato, N., Lei, X., Wen, X., 2007. A synthetic seismicity model for the Xianshuihe fault, southwestern China, simulation using a rate- and state-dependent friction law. Geophysical Journal International 169, 286–300.

King, R.W., et al., 1997. Geodetic measurement of crustal motion in southwest China. Geology 25 (2), 179–182.

Kirby, E., et al., 2007. Slip rate gradients along the eastern Kunlun fault. Tectonics 26 (TC2010). doi:10.1029/2006TC002033.

Lin, A., Guo, J., 2008. Nonuniform slip rate and millennial recurrence interval of large earthquakes along the eastern segment of the Kunlun Fault, Northern Tibet. Bulletin of the Seismological Society of America 98 (6), 2866–2878. doi:10.1785/0120070193.

Liu, M., Yang, Y., 2003. Extensional collapse of the Tibetan Plateau: results of three-dimensional finite element modeling. Journal of Geophysical Research—Solid Earth 108 (82361).

Liu, M., Yang, Y., Stein, S., Zhu, Y., Engeln, J., 2000. Crustal shortening in the Andes: why do GPS rates differ from geological rates? Geophysical Research Letters 27, 3005–3008.

Liu, R., et al., 2006. Comparison between earthquake magnitudes determined by China seismograph network and U.S. seismograph network (2): surface wave magnitude (in Chinese). Acta Geologica Sinica 28 (1), 1–7.

Luo, G. and Liu, M., 2009-this volume. Stress evolution and fault interactions in eastern Tibet: implications for the 2008 Mw7.9 Wenchuan earthquake. Tectonophysics.

Meade, B.J., 2007. Present-day kinematics at the India–Asia collision zone. Geology 35 (1), 81–84. doi:10.1130/G22924A.1.

Meade, B.J., Hager, B.H., 2005a. Block models of crustal motion in southern California constrained by GPS measurements. Journal of Geophysical Research—Solid Earth 110 (B03403). doi:10.1029/2004JB003209.

Meade, B.J., Hager, B.H., 2005b. Spatial localization of moment deficits in southern California. Journal of Geophysical Research—Solid Earth 110 (B4).

Meade, B.J., et al., 2002. Estimates of seismic potential in the Marmara Sea region from block models of secular deformation constrained by global positioning system measurements. Bulletin of the Seismological Society of America 92 (1), 208–215.

Molnar, P., Tapponnier, P., 1977. The collision between India and Eurasia. Science American 236 (4), 30–41.

Molnar, P., Lyon-caen, H., 1989. Fault plane solutions of earthquakes and active tectonics of the Tibetan Plateau and its margins. Geophysical Journal International 99, 123–153.

Okada, Y., 1985. Surface deformation due to shear and tensile faults in a half-space. Bulletin of the Seismological Society of America 75, 1135–1154.

Papadimitriou, E., Wen, X., Karakostas, V., Jin, X., 2004. Earthquake triggering along the Xianshuihe fault zone of western Sichuan, China. Pure and Applied Geophysics 161, 1683–1707.

Parsons, T., Ji, C., Kirby, E., 2008. Stress changes from the 2008 Wenchuan earthquake and increased hazard in the Sichuan basin. Nature 454 (7203), 509–510. doi:10.1038/nature07177.

Peltzer, G., Crampe, F., King, G., 1999. Evidence of nonlinear elasticity of the crust from the Mw7.6 Manyi (Tibet) earthquake. Science 286 (5438), 272–276.

Qin, C., Papadimitriou, E.E., Papazachos, B.C., Kapakaisis, G.F., 1999. Spatial distribution of time-independent seismicity in China. Pure and Applied Geophysics 154, 101–119.

Ran, H., He, H., 2006. Research on the magnitude and recurrence interval of characterized earthquakes with magnitude >6.7 along the northwestern portion of the Xianshuihe fault zone in western Sichuan, China (in Chinese). Chinese. Journal of Geophysics 49 (1), 153–161.

Replumaz, A., Tapponnier, P., 2003. Reconstruction of the deformed collision zone between India and Asia by backward motion of lithospheric blocks. Journal of Geophysical Research—Solid Earth 108 (B6).

Royden, L.H., Burchfiel, B.C., Hilst, R.D.v.d., 2008. The geological evolution of the Tibetan Plateau. Science 321, 1054–1058. doi:10.1126/science.1155371.

Savage, J.C., Burford, R.O., 1973. Geodetic determination of relative plate motion in central California. Journal of Geophysical Research—Solid Earth 78 (5), 823–845.

Shen, Z.K., Zhao, C., Yin, A., Jackson, D., 2000. Contemporary crustal deformation in east Asia constrained by Global Positioning System measurements. Journal of Geophysical Research—Solid Earth 105, 5721–5734.

Shen, Z., Lv, J., Wang, M., Burgmann, R., 2005. Contemporary crustal deformation around the southeast borderland of the Tibetan Plateau. Journal of Geophysical Research—Solid Earth 110 (B11409). doi:10.1029/2004JB003421.

Swafford, L., Stein, S., 2007. Limitations of the short earthquake record for seismicity and seismic hazard studies. In: Stein, S., Mazzotti, S. (Eds.), Continental Intraplate

Please cite this article as: Wang, H., et al., Balance of seismic moment in the Songpan-Ganze region, eastern Tibet: Implications for the 2008 Great Wenchuan earthquake, Tectonophysics (2009), doi:10.1016/j.tecto.2009.09.022

Earthquakes: Science, Hazard, and Policy Issues: Geological Society of America Special Paper, vol. 425, pp. 49–58. doi:10.1130/2007.2425(04).
Tapponnier, P., et al., 2001. Oblique stepwise rise and growth of the Tibet Plateau. Science 294 (5547), 1671–1677.
Thatcher, W., 2007. Microplate model for the present-day deformation of Tibet. Journal of Geophysical Research—Solid Earth 112 (B01401).
Toda, S., Lin, J., Meghraoui, M., Stein, R.S., 2008. 12 May 2008 M = 7.9 Wenchuan, China, earthquake calculated to increase failure stress and seismicity rate on three major fault systems. Geophysical Research Letters 35 (L17305). doi:10.1029/2008GL034903.
Van der Woerd, J., et al., 2000. Uniform slip-rate along the Kunlun Fault: implications for seismic behaviour and large-scale tectonics. Geophysical Research Letters 27 (16), 2353–2356.
Van der Woerd, J., et al., 2002. Uniform postglacial slip-rate along the central 600 km of the Kunlun Fault (Tibet), from Al-26, Be-10, and C-14 dating of riser offsets, and climatic origin of the regional morphology. Geophysical Journal International 148 (3), 356–388.
Vigny, C., et al., 2003. Present-day crustal deformation around Sagaing fault, Myanmar. Journal of Geophysical Research—Solid Earth 108 (B112533). doi:10.1029/2002JB001999.
Wallis, S., et al., 2003. Cenozoic and Mesozoic metamorphism in the Longmenshan orogen: implications for geodynamic models of eastern Tibet. Geology 31 (9), 745–748.
Wang, E., et al., 1998. Late Cenozoic Xianshuihe-Xiaojiang, Red River, and Dali Fault systems of Southwestern Sichuan and Central Yunnan, 327. China, Geological Society of American Special Paper.
Wang, Q., et al., 2001. Present-day crustal deformation in China constrained by global positioning system measurements. Science 294, 574–577.
Wang, C., Han, W., Wu, J., Lou, H., Bai, Z., 2003. Crustal structure beneath the Songpan-Garze Orogenic belt (in Chinese). Acta Seismologica Sinica 25 (3), 229–241.
Wang, C., Han, W., Wu, J., Lou, H., Chan, W.W., 2007. Crustal structure beneath the eastern margin of the Tibetan Plateau and its tectonic implications. Journal of Geophysical Research—Solid Earth 112 (B07307). doi:10.1029/2005JB003873.
Wang, C.Y., Flesch, L.M., Silver, P.G., Chang, L.J., Chan, W.W., 2008a. Evidence for mechanically coupled lithosphere in central Asia and resulting implications. Geology 36 (5), 363–366. doi:10.1130/G24450A.1.
Wang, Y., et al., 2008b. GPS-constrained inversion of present-day slip rates along major faults of the Sichuan-Yunnan region, China. Science in China (Series D) 51 (9), 1267–1283.
Wen, X., Yi, G., Xu, X., 2007. Background and precursory seismicities along and surrounding the Kunlun fault before the Ms8.1, 2001, Kokoxili earthquake, China. Journal of Asian Earth Sciences 30, 63–72.
Wen, X., Ma, S., Xu, X., He, Y., 2008. Historical pattern and behavior of earthquake ruptures along the eastern boundary of the Sichuan-Yunnan faulted-block, southwestern China. Physics of the Earth and Planetary Interiors 168, 16–36.
Woerd, J.V.d., et al., 2000. Uniform Slip Rate along the Kunlun Fault: implications for seismic behaviour and large-scale tectonics. Geophysical Research Letters 27 (16), 2353–2356.
Xu, X., Wen, X., Chen, G., Yu, G., 2008. Discovery of the Longriba fault zone in eastern Bayan Har Block, China and its tectonic implication. Science in China Series D—Earth Sciences 51 (9), 1209–1223.
Yang, Z.X., Waldhauser, F., Chen, Y.T., Richards, P.G., 2005. Double-difference relocation of earthquakes in central-western China, 1992–1999. Journal of Seismology 9 (2), 241–264.
Yi, G., Wen, X., Xu, X., 2002. Study on recurrence behaviors of strong earthquakes for several entireties of active fault zones in Sichuan-Yunnan region (in Chinese). Earthquake Research in China 18 (3), 267–276.
Zhang, P., Yang, Z., Gupta, H.K., Bhatia, S.C., Shedlock, K.M., 1999. Global seismic hazard assessment program (GSHAP) in continental Asia. ANNALI DI GEOFISICA 42 (6), 1167–1190.
Zhang, P., et al., 2003. Active tectonic blocks and strong earthquakes in the continent of China. Science in China Series D—Earth Sciences 46 (Supplement), 13–24.
Zhang, P.Z., et al., 2004. Continuous deformation of the Tibetan Plateau from global positioning system data. Geology 32 (9), 809–812.
Zhang, G., Ma, H., Wang, H., Wang, X., 2005. Boundaries between active-tectonic blocks and strong earthquakes in the China mainland (in Chinese). Chinese Journal of Geophysics 48 (3), 602–610.
Zhang, P., Molnar, P., Xu, X., 2007. Late Quaternary and present-day rates of slip along the Altyn Tagh Fault, northern margin of the Tibetan Plateau. Tectonics 26 (TC5010). doi:10.1029/2006TC002014.
Zhang, P., Xu, X., Wen, X., Ran, Y., 2008. Slip rates and recurrence intervals of the Longmen Shan active fault zone, and tectonic implications for the mechanism of the May 12 Wenchuan earthquake, 2008, Sichuan, China (in Chinese). Chinese Journal of Geophysics 51 (4), 1066–1073.
Zhou, R.J., et al., 2007. Active tectonics of the Longmen Shan region on the eastern margin of the Tibetan plateau. Acta Geologica Sinica—English Edition 81 (4), 593–604.

Please cite this article as: Wang, H., et al., Balance of seismic moment in the Songpan-Ganze region, eastern Tibet: Implications for the 2008 Great Wenchuan earthquake, Tectonophysics (2009), doi:10.1016/j.tecto.2009.09.022